Research on Engineering Structures & Materials
www.jresm.org

Research Article

Development of eco-friendly concrete paving blocks utilizing one-part alkali-activated binders

Sujeet Kumar [*,a], Ajay Kumar Sinha [b]

Department of Civil Engineering, National Institute of Technology, Patna, 800005, India

Article Info

Article History:

Received 12 June 2025

Accepted 25 Aug 2025

Keywords:

Concrete paving blocks;
Alkali-activated binder;
One-part;
Strength;
Durability;
Sustainability

Abstract

The growing population has led to increased construction needs in the developing nations, with demands for better pedestrian and non-motorized pavement infrastructure. Such infrastructure requires low material strength, which offers an opportunity to utilize innovative binders from industrial waste. Therefore, this study explores concrete paving blocks with one-part alkali-activated binders (AAB), formulated using ground granulated blast furnace slag (GGBS), to create a substitute for conventional blocks with lower carbon footprints and economic advantages. GGBS was mixed with solid sodium metasilicate (SMS) and calcium hydroxide (CH) in three different SMS/CH ratios as 2.33, 1.50, and 1.00. M35 grade concrete mixes were employed to prepare the paving blocks, suitable for light traffic applications. Using standard techniques, the strength and durability characteristics of the blocks were evaluated under consideration of mechanical strengths, density, water absorption, resistance to abrasion, and strength loss under acid attack. These outcomes were then compared with those of traditional paving blocks. All AAB blocks achieved the specified requirements in strength and durability as per the standard. Most importantly, AAB-1 blocks, which were produced using 80% GGBS, 14% SMS, and 6% CH as binder, surpassed the strength and durability performances of traditional paving blocks. AAB blocks are eco-friendly, with carbon emissions reduced by 59% and the cost of production by 15-23%. AAB blocks typically address environmental issues and realize cost savings for sustainable construction in low-traffic pavement applications.

1. Introduction

The need for construction across industrial, commercial, and residential areas has increased in tandem with global population growth. Governments in developing countries are promoting urbanization through various infrastructure and development projects. In India, which has the second-largest population, the significance of pavement infrastructure is rising due to insufficient facilities for pedestrians and non-motorized transport [1]. As a result, the demand for construction units like paving blocks is likewise growing in these regions. Concrete paving blocks, is a non-reinforced pre-cast blocks used in diverse pavements like driveways, parking areas, paths, roads, streets, and industrial sites [2]. They are generally manufactured of cement, aggregates, water, admixtures, and color pigments. The production of concrete paving blocks is expected to increase further by 4.9 % worldwide from 2020 to 2032 [3]. This growing production of blocks brings up environmental concerns, as it indicates a heightened demand for cement. The energy-intensive processes of clinker production and calcination process involved in production of cement contribute to approximately 7–8% of total man-made carbon emissions [4]. For many decades, cement manufacturers have been producing blended cements to tackle issues like reduction in cost, energy use, and lowering carbon emissions. Portland pozzolana cement is identified as the most

*Corresponding author: sujeetk.ph21.ce@nitp.ac.in
[a]orcid.org/0000-0002-9875-2248; [b]orcid.org/0000-0002-2265-3008
DOI: http://dx.doi.org/10.17515/resm2025-963ma0612rs

popular type, making up about 70% of total cement produced in India [5]. Portland slag and composite cements are other recognized variants of blended cements. Despite these efforts, the cement industry is accountable for a very high carbon emission, which emphasizes the urgent requirement to develop alternative binders for the construction sector. An alternative binder using industrial by-products, such as alkali-activated binder (AAB), offers a promising way to significantly lower carbon emissions and has been vastly studied by researchers in the previous two decades. Therefore, the concrete paving blocks should be investigated using AAB and differentiate with the conventional blocks.

The development of AAB involves activating solid alumino-silicate materials such as GGBS, fly ash (FA), and similar materials by alkaline liquid activators. Various liquid alkaline activator combinations are employed in the production of AAB, and due to the separate preparation of the alkaline solution, it is termed as two-part AABs [6–8]. In contrast, one-part AAB offers a new and exciting way to simplify the mixing process with a simple just-add-water approach. By minimizing exposure to toxic chemicals, this new technique not only enhances productivity on site but also provides safety [9–11]. The mixture consists of a stable alkali activator with a dry blend of alumino-silicate precursor; water is the sole extra requirement for the manufacture of a binding paste. Relative to other alumino-silicate materials, GGBS, which is an industrial by-product, improves durability, reduces permeability, and shows improved mechanical properties [12–16]. This is mainly because GGBS has high reactivity and the presence of amorphous phases, which play a major role in the production of AABs. The significant presence of calcium oxide, silicon oxide, and aluminium oxide facilitates the formation of calcium aluminium silicate hydrate (C-A-S-H) gel during the production of AABs [17]. It is compatible with various activators, and it develops adequate strength under both ambient and water curing, in addition to exhibiting excellent durability properties. Such a property makes GGBS an excellent candidate material for one-part AABs. While sodium metasilicate (SMS) is a good activator for one-part AABs [18,19], it is with some limitations, such as rapid setting times, efflorescence, and cracking susceptibility [20–22]. Additionally, understanding the role of calcium hydroxide (CH) in alkali-activation system is essential, since the addition of CH along with the main activators is capable of enhancing the binder performance [23]. Research into these materials has the ability to upgrade sustainability, safety, and structural resistance in the construction industry; hence, an increased understanding of these materials will be capable of optimizing formulation as well as performance of AABs.

Literature suggests that the strength and durability characteristics of concrete paving blocks were majorly investigated employing two-part AABs [24–29]. Recent work has highlighted the potential of various industrial by-products, such as GGBS, FA, and rice husk ash, in the production of high-quality paving blocks. The mixture of sodium silicate (SS) and sodium hydroxide (SH) solutions was commonly adopted as liquid activators in two-part AABs for activation. Mahdi et al. [24] carried out a study on paver blocks using two-part AABs that incorporated rice husk ash from brick kilns along with a combination of SS and SH solutions. The paving blocks satisfy the requirements set by IS 15658–2021 [30], gaining compressive strength (CS) from 30.4 to 42.7 MPa, tensile splitting strength (TSS) in range of 2.2-3.2 MPa, and flexural strength (FS) in range of 4.1-7.6 MPa. The paving blocks showed water absorption ranging 3.8 to 5.6%, and the strength loss upon acid attack varied from 2.2% to 4.8% after 28 days. Previous studies [2] on concrete paver blocks that incorporated fly ash and GGBS found CS reaching up to 57.53 MPa in just 7 days, fulfilling M40 and M50 grades, with minimal water absorption and enhanced abrasion resistance. Paving blocks made with FA [31] demonstrated TSS between 3.0 and 3.8 MPa, along with impressive durability features. Under ambient curing conditions, Revathi et al. [25] obtained CS of 57.34-59.58 MPa and very low water absorption in the case of M30 and M35 grades using bottom ash and GGBS as solid precursors. Conversely, the application of one-pat AABs in the fabrication of concrete paving blocks has been the subject of some research. For instance, Rashid et al. [18] produced one-part AAB blocks with GGBS having CS of 19-28 MPa. The blocks were especially suitable for low-strength structural blocks. In another research by Jameel et al. [19], mixing FA, GGBS, recycled aggregates, and plastic yielded pedestrian blocks with FS ranging from 3.7 to 5.1 MPa and CS ranging from 13.2 to 18.7 MPa. The blocks meet the durability requirement and lowered carbon emissions by 70%. Together, these results highlight the versatility and environmental-friendliness of one-part AABs

in the manufacture of concrete paving blocks. This demonstrates their ability to fulfill the structural requirements, environmental needs, and economy in the current construction practice.

1.1. Research Significance

In the context of concrete paving blocks, numerous research studies in the area of alkali-activated materials particularly focus on two-part AABs. There have been very limited investigations on the development of paving blocks using one-part AABs, particularly those designed for various pavement applications. Literature suggests that one-part AABs are considered safer than two-part AABs, as they eliminate the requirement of handling corrosive liquid alkaline solutions. Two-part systems need a separate liquid alkaline activator, which is extremely corrosive and requires strict safety precautions. On the other hand, one-part systems employ dry powder activators, which are blended in with the alumino-silicate precursor. This simplifies the handling process and reduces safety risks, which makes it a similar process to that of traditional concrete. Therefore, this investigation involves investigating the essential characteristics of concrete paving blocks prepared using one-part AABs. GGBS blended with solid SMS and CH was employed as a binder for the manufacture of concrete paving blocks. The activator ratio (SMS/CH) was kept at 2.33, 1.50, and 1.00 to prepare three different mixtures for paving blocks. The mix proportion of concrete was formulated to produce M35 grade paving blocks, which are suitable for pedestrian and low-traffic pavement use. The present research examined the fundamental characteristics of paving blocks, specifically their compressive strength, tensile splitting strength, flexural strength, water absorption, and abrasion resistance in accordance with the Indian standard code IS 15658–2021 [30]. Additionally, an acid resistance test was performed to analyze the performance of the blocks under extreme acidic conditions. Environmental impact analysis and cost estimation were also carried out to establish the carbon footprint and cost of production of AAB blocks compared to conventional blocks. The resulting AAB blocks were found suitable for M35 grade paving application with low carbon footprint and additional cost benefits.

2. Materials and Experimental Methods

2.1. Materials

2.1.1. Solid Precursor and Alkali Activators

In this work, GGBS as an alumino-silicate precursor was used, while a combination of solid sodium metasilicate anhydrous (SMS) and calcium hydroxide (CH) was used as the alkaline activators. The GGBS with a specific gravity of 2.85 was supplied by Astrra Chemicals, Chennai, India. The SMS (Na_2SiO_3), in its granular form with a molar ratio of SiO_2/Na_2O=0.9, and the CH in fine powder form, containing $Ca(OH)_2$ with 96% purity and a bulk density of 2.21 g/mL, were sourced from Akshar Chem Exim Co. Pvt Ltd, Kolkata, India.

2.1.2. Binders

This experimental study was conducted on three one-part AABs used in the preparation of concrete paving blocks. All these binders consisted of 80% GGBS and 20% a blend of solid activators, as detailed in Table 1. According to the results of preliminary examination and prior research in this field [10,18,32], the activators were set on the basis of the weight of total solids at 20%. Within this investigation, a supplementary activator was employed due to the limitations of GGBS activation using SMS alone. Prior research indicated that escalating the SMS content as an activator in one-part AABs raised several durability-related issues, including efflorescence formation and micro-cracks [20,22]. Therefore, the binders included 80% GGBS and 20% a mixture of SMS and CH as activators. The binders were prepared by homogeneously dry mixing GGBS with the appropriate blend of solid activators before use. A digital mechanical mixer was employed to mix the components for a period of 3-5 minutes to get a homogeneous mixture. The prepared binders were stored in sealed bags for subsequent use. Additionally, for comparative analysis of binder performance, Composite Cement (CC) was acquired from the market and utilized in this assessment. CC conforms to IS 16415:2015 [33], considered equivalent to 33-grade ordinary Portland cement (OPC), and primarily comprises OPC, FA, and GGBS. The CC sourced was a blend

containing 32.50% FA, 30.25% GGBS, and the remaining 37.25% OPC (neglecting gypsum content; data as per the supplier).

Table 1. Composition of the binding mixture for binders in each 50-kilogram bag of binder

Mix ID	Binder mix ratio	Mass proportions per 50 kg bag (in kg)		
		GGBS	SMS	CH
AAB-1	80% GGBS + 14% SMS + 6% CH	40	07	03
AAB-2	80% GGBS + 12% SMS + 8% CH	40	06	04
AAB-3	80% GGBS + 10% SMS+ 10% CH	40	05	05

2.1.3. Aggregate and Water

The river sand, available locally and adhering to Zone III of IS 383:2016 [34], served as the fine aggregate. Through laboratory experiments, coarse aggregates comprising 12.5 mm and 10 mm nominal sizes were combined in a 60 % to 40 % proportion to produce a well-graded coarse aggregate of 12.5 mm nominal size, in accordance with IS 383:2016 [34]. In line with the guidelines of IS 456:2000 [35], potable water was utilized for preparing test samples.

2.2. Mix Composition and Preparation of Concrete Paving Blocks

In light of the observed performance of various binders, concrete paving blocks were formed utilizing all these binders to conduct a comparative study. The mix proportion was formulated in accordance with the guidelines of IS 10262:2019 [36], with the objective of achieving a CS of 35 MPa at 28-days for concrete paving blocks. The water to binder (w/b) ratio was modified for attaining the required workability. The concrete mix ratios were carefully determined, ensuring that all binders matched the specifications of 33-grade OPC. The final mix ratios settled on were 1 part binder, 1.45 parts fine aggregate, and 2.65 parts coarse aggregate, with a w/b ratio of 0.40, based on initial lab tests. The maximum binder content was retained at 450 kg/m^3, and the w/b of 0.40 was set to achieve concrete mixes with zero to low slump and produce high-strength paving blocks. Table 2 elucidates the detailed mix proportions of the concrete blends used for manufacturing the paving blocks. The goal was to create M35 grade concrete suitable for paving blocks intended for light traffic, as specified in IS 15658: 2021 [30]. Additionally, the standard called for a minimum thickness of 60 mm for these M35 grade concrete paving blocks. For this, PVC molds of zig-zag pattern whose size was 265 mm x 120 mm x 60 mm were utilized to cast the pavers blocks (see Figure 1a).

For the preparation of paving blocks, the provided proportions of binder, sand, and coarse aggregate were mixed for 2 minutes in dry form by a laboratory pan-type mixer. Next, the measured amount of water, as determined from the w/b ratio, was added to the mix, and further mixing was done for an additional 3-5 minutes in order to achieve a homogeneous concrete mix (Figure 1b). During mixing and casting operations, the temperature and relative humidity were kept at 27 ± 2 °C and 65 ± 5%, respectively, within the laboratory environment. The concrete mix was poured into the PVC molds size 265 mm x 120 mm x 60 mm (shown in Figure 1c) immediately after preparation. These molds were compacted with a table vibrator. Post-compaction, the cast molds were covered by a damp cloth and kept in the lab conditions for 24 ± 2 h. Subsequently, the paving blocks were demolded (Figure 1d) and kept under water at 27 ± 2 °C temperatures in a curing tank until they reached the designated age for various evaluations.

Table 2. Compositions of concrete mixes used in the production of paving blocks

Mix ID	GGBS (kg/m^3)	SS (kg/m^3)	CH (kg/m^3)	CC (kg/m^3)	Fine aggregate (kg/m^3)	Coarse Aggregate (kg/m^3)	Water (kg/m^3)
CC	-	-	-	450	652.5	1192.5	180
AAB-1	360	63	27	-	652.5	1192.5	180
AAB-2	360	54	36	-	652.5	1192.5	180
AAB-3	360	45	45	-	652.5	1192.5	180

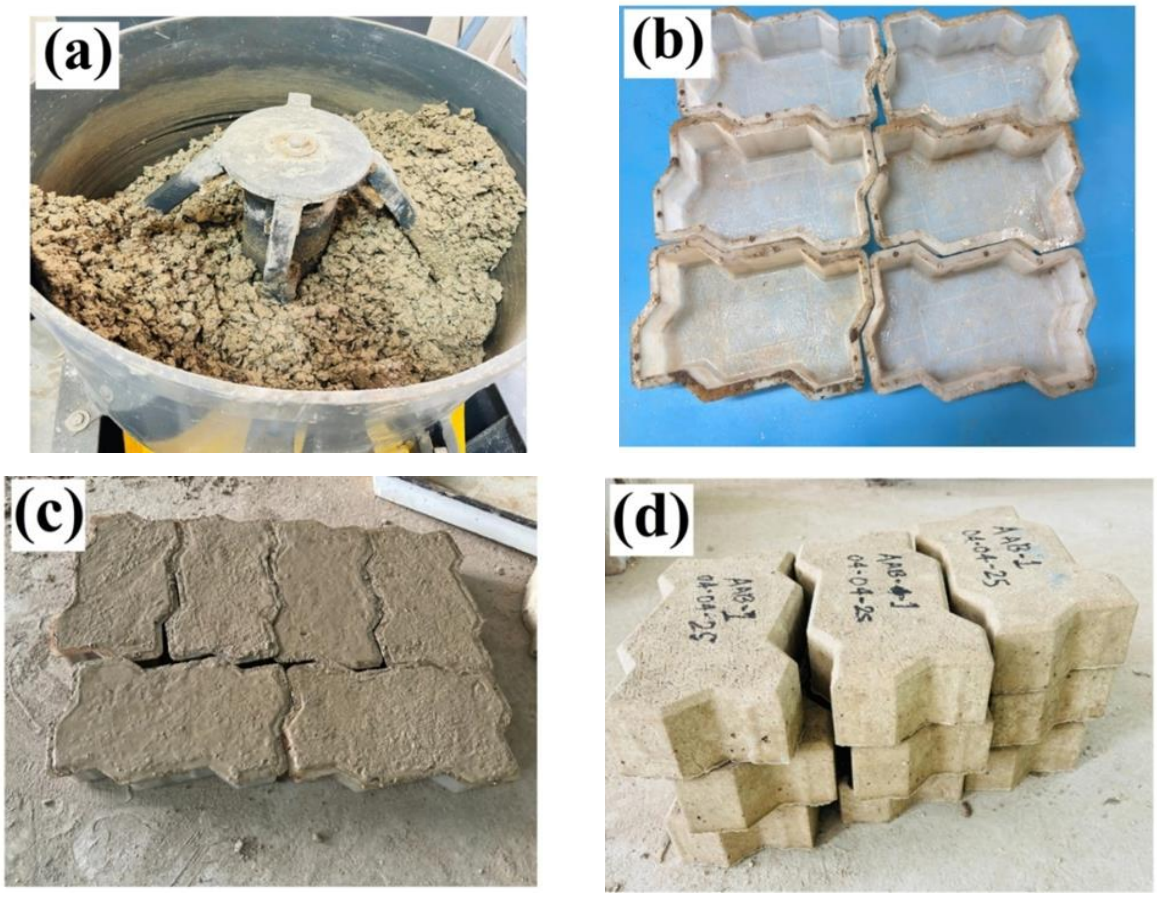

Fig. 1. Concrete paving block production- (a) freshly prepared concrete, (b) PVC zigzag molds, (c) molds filled recently, and (d) paving units after removal from molds

2.3. Experimental Methods

2.3.1. Characterization of Starting Materials

The chemical composition of GGBS was analyzed with the help of an X-ray fluorescence spectrometer (Rigaku NEX DE, USA). The mineralogical characteristics of GGBS were analyzed using an X-Ray Diffractometer (Shimadzu XRD-7000, Japan) with CuKα radiation at a scanning speed of 4° 2θ/min and sampling pitch of 0.02° to scan the GGBS powder sample in the range of 10° to 80° 2θ angle. For the determination of particle size distribution of GGBS and CH, a laser-diffraction particle size analyzer (Horiba SZ-100, Japan) was utilized. In contrast, the particle size of SMS was determined using the sieving method due to its coarser size. Blaine's air permeability method, as per the procedure mentioned in IS 1727:1967 [37], was used to determine the fineness of GGBS, SMS, and CH. The sieve analysis for fine and coarse aggregates was performed in accordance with IS 2386 (Part I):1963 [38]. The specific gravity of aggregates was determined as per IS 2386 (Part 3):1963 [39].

2.3.2. Assessment of Binder Performance

The efficacy of the binders was evaluated to verify their equivalence to 33-grade OPC. The testing protocols for the binders adhered to methodologies akin to those detailed in Table 3. Throughout the testing process, the ambient conditions of the laboratory were kept at a temperature of 27 ± 2 °C and a relative humidity of 65 ± 5%. Potable water was employed during the preparation of paste and mortar specimens for these assessments. Paste and mortar mixes were prepared using a mechanical mortar mixer for casting molds.

To assess CS, mortar mixtures were formulated using a proportion of 1 part binder to 3 parts sand, along with water according to the standard consistency. Specimens were cast into steel molds in the form of cubes measuring 70.6 mm, employing a vibration machine. A digital compression

testing machine was utilized for measuring the CS of all binders. All test samples were put through underwater curing using a curing tank until the designated age of the test.

Table 3. Methodologies employed for assessing binder performance

Name of test	Sample	Parameters obtained	Methods
Fineness test	Binder	Blaine's fineness (m^2/kg)	IS 4031(Part 2)-1988 [40]
Standard consistency test	Paste	Standard consistency (P %)	IS 4031(Part 4)-1988 [41]
Setting time test	Paste	Initial and final setting times (minutes)	IS: 4031(Part 5)-1988 [42]
Compressive strength test	Mortar	Compressive strength at 3, 7, 28 days	IS: 4031(Part 6)-1988 [43]
Soundness test	Paste	Le-chatelier expansion (mm)	IS: 4031 (Part 3)-1988 [44]

2.3.3. Test on Hardened Concrete Paving Blocks

The evaluations of concrete paving blocks' performance were conducted following the procedures described in IS 15658: 2021 [30]. Throughout all trials, the environmental conditions in the laboratory were kept at a temperature of 27 ± 2 °C and a relative humidity of 65 ± 5%. Visual inspection, assessment of shape, and measurement of dimensions were conducted on 08 paving blocks from each concrete mix, following the standard. The plan area of the pavers was established using Method 2 as per Annex B of the standard.

The compressive strength (CS), tensile splitting strength (TSS), and flexural strength (FS) of the paving blocks were assessed at intervals of 3, 7, 14, and 28 days of curing, utilizing methods outlined in Annex D, Annex F, and Annex G of IS 15658:2021, respectively [30]. These tests were performed using a digital compression testing machine (AIM-317E-MU-1-T, AIMIL, India) using various test attachments. For each evaluation period, three samples were subjected to a compression test (Figure 2a), and the mean test result was recorded. The CS was obtained by taking the ratio of peak load (N) to the plan area of the blocks (mm^2). The test result calculated was then adjusted using a recommended correction factor (k = 1.06, for 60 mm thick zig-zag paving blocks) to acquire corrected CS values across all test periods.

Regarding the TSS, the paving block was positioned on the testing device such that the packing pieces were situated on the upper and lower surfaces, coming into contact with the supports of the split test fixture (Figure 2b). The sample was loaded until failure, and the TSS was determined using equation (1).

$$T = 0.637.k.P/S \quad (1)$$

Where, T = TSS (MPa), P = failure load (N), S= cross-sectional area of the failure plane of the test sample (mm2), k = correction factor for block thickness = 0.87; for 60 mm thick paving blocks as per Annex F of the standard.

To assess the FS, the paving block was positioned in a simply supported manner upon two solid cylindrical rollers, while a central force was exerted using a third roller, as depicted in Figure 2c. The sample underwent a load application until rupture, and the FS of the paving blocks was determined by equation (2).

$$F_b = 3PL/(2bd^2) \quad (2)$$

Where, F_b = FS (MPa), P = ultimate load (N), L = centre to centre length between two rollers (mm), b = mean width of block assessed from both specimen faces (mm), d = mean thickness assessed from both fracture lines' ends (mm).

The density of hardened paving blocks was ascertained by applying the mass-to-volume ratio on samples from each group after they had undergone 28 days of curing. The mean from three test samples was utilized to derive the densities for all paving blocks. Subsequently, the water absorption of these blocks was evaluated as per Annex C, IS 15658:2021 [30]. The blocks were

immersed in water for 24 ± 2 h, accompanied by heating in an electric oven set at 105 ± 5 °C. The test was conducted on three blocks from each mix type to find the mass loss (%) of the specimens.

The abrasion resistance of paving blocks was done using the procedure recommended in Annex E, IS 15658:2021 [30]. A square sample measuring 70±0.1 mm cross-section and thickness of 50 mm was extracted from the broken test pieces of 28 days' flexural strength test. The sample was subsequently tested in a dry state using an abrasion testing apparatus. The test sample was loaded centrally with a load of 294±3 N. The revolution of grinding disc was set at 30 rpm and the disc was halted after one-cycle comprising 22 rotations. This test-cycle was repeated 16-times, with the square sample being rotated 90° clockwise and about 20g of abrasive powder was distributed over the testing path after every test-cycle. The abrasive resistance of blocks was determined as an average volume loss of test sample (mm^3 per 5000 mm^2).

To assess the durability in an acidic environment, the hardened paving blocks, after 28-days of curing, were submerged in a 5% H_2SO_4 solution for the acid attack resistance test. Sulfuric acid (H_2SO_4) with 98% purity (manufacturer - Merk Ltd.) was sourced locally for this evaluation. The test procedure was adopted as described in earlier research [24]. Three paving blocks from each batch were immersed in an acidic solution, kept in a sealed container. The pH value of 2 for acid solution was maintained during the experiment. The samples were air dried in lab conditions of 27 ± 2 °C and relative humidity of 65 ± 5% for 72±2 h after immersion. The durability of the blocks was evaluated by quantifying the loss in CS of the paving blocks following acid exposure of 28 days.

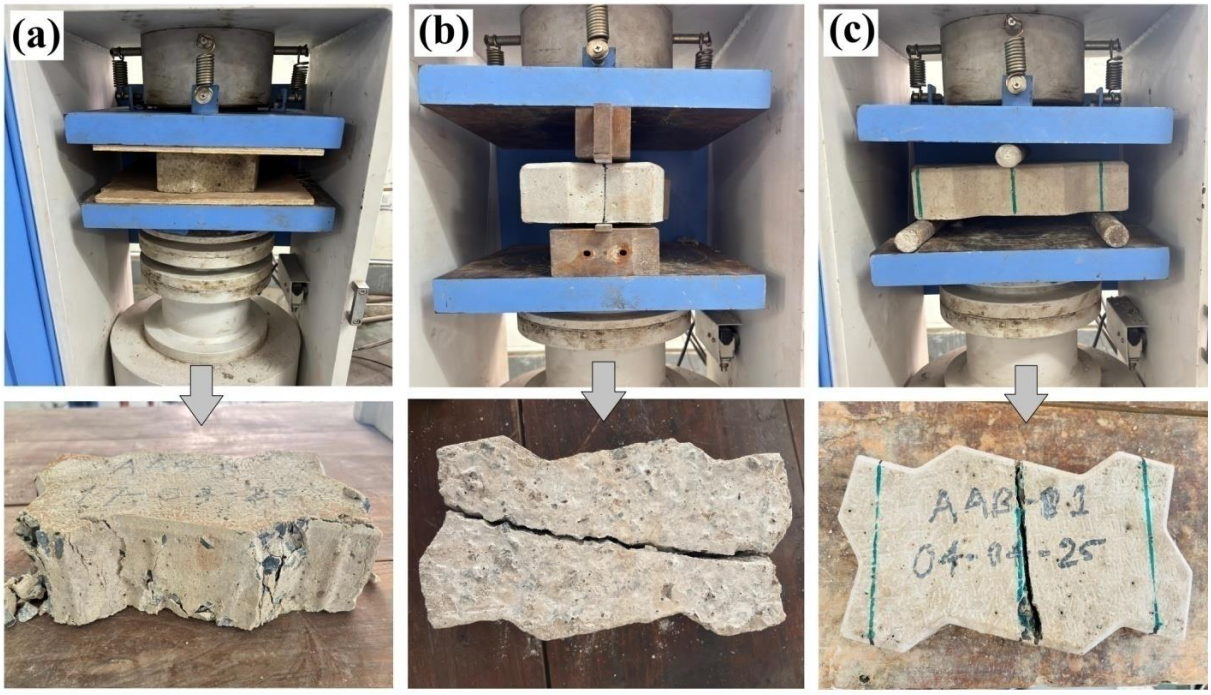

Fig. 2. Testing setup used for the (a) compressive strength, (b) tensile splitting strength, and (c) flexural strength tests, and the resulting failure modes for specimens under each respective test

3. Results and Discussion

3.1. Characteristics of Starting Materials

The result of the XRF analysis of GGBS is shown in Table 4, which indicates that GGBS is a calcium-rich material, containing 42.7% calcium oxide content. SiO_2 and Al_2O_3 are other predominant oxides in GGBS, accounting for 31.2 % and 15.1 % respectively. Furthermore, XRD analysis (Figure 3) confirmed that the GGBS was largely non-crystalline, a characteristic suggested by the absence of distinct peaks usually associated with crystalline materials. A broad hump in the range of 25° to 35° 2θ angle represents the amorphous structure of minerals present in it [45]. The particle size

distribution curves for GGBS and the solid activators are depicted in Figure 4. The median particle diameters (d_{50}) were determined to be 13.85 μm for GGBS, 575 μm for SMS, and 11.75 μm for CH.

Table 4. Chemical composition of GGBS

Constituents	CaO	SiO_2	Al_2O_3	MgO	MnO	SO_3	TiO_2	Fe_2O_3	K_2O	LOI
(%)	42.7	31.2	15.1	5.71	1.63	1.19	1.11	0.68	0.46	0.26

Blaine fineness tests yielded values of 420 m^2/kg, 151 m^2/kg, and 450 m^2/kg for GGBS, SMS, and CH, respectively. The Blaine fineness values for GGBS, SMS, and CH came in at 420, 151, and 450 m^2/kg, respectively. This analysis indicates that the SMS granules are noticeably coarser, while the CH shows a much finer texture compared to GGBS. The properties of SMS, as provided by the manufacturer, are presented in Table 5.

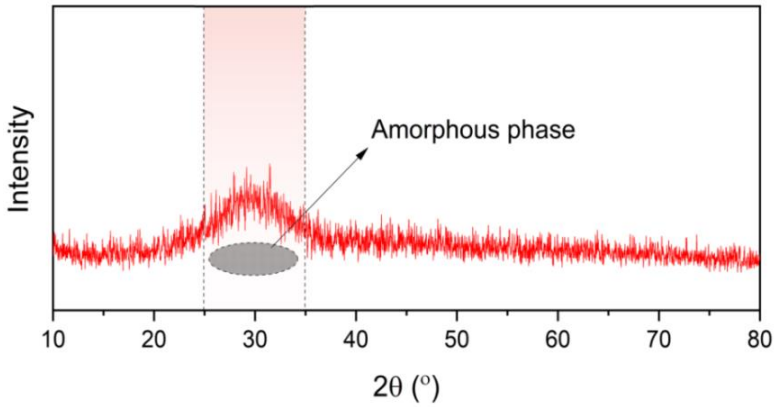

Fig. 3. XRD pattern of GGBS used in this study

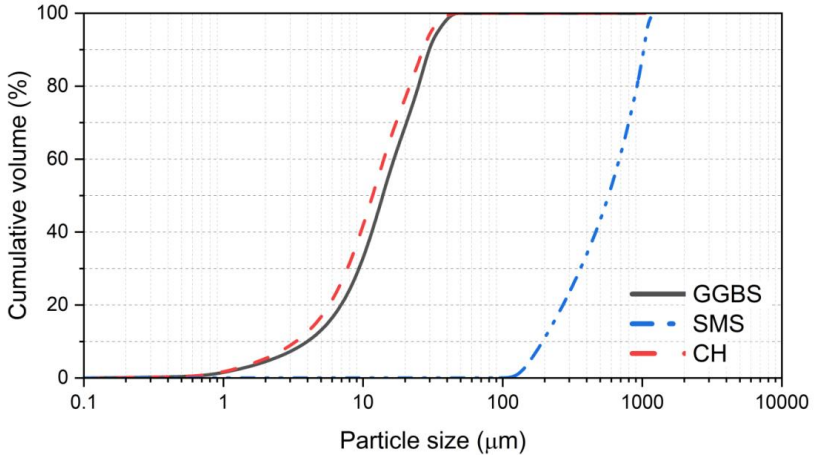

Fig. 4. Particle size distribution curves for GGBS, SMS, and CH

Table 5. Properties of anhydrous sodium metasilicate

Descriptions	Results
Na_2O (%)	50-52
SiO_2 (%)	≥48
Modulus	0.9
Water insoluble	< 0.3 %
pH in 1% solution	12.6 ± 0.2
Bulk density (g/mL)	1.05 ± 0.17

The data suggest that SMS has a low SiO_2/Na_2O ratio of 0.9, which is considered beneficial, as a low modulus ratio indicates less polymerized silica and, thus, shows faster dissolution for the

production of GGBS-based one-part AABs [46]. The faster dissolution contributes to achieving the high early strength of the developed products. The physical attributes of fine and coarse aggregates used in the preparation of concrete paving blocks for all mixes are detailed in Table 6.

Table 6. Fine and coarse aggregate characteristics

Parameters		Fine Aggregate	Coarse Aggregate	Remarks
Sieve Analysis	Sieve Size	% Passing	% Passing	
	20 mm	-	100	River sand of grading zone-III (conforms to Table 9 of IS 383:2016 [34] and Graded coarse aggregate of nominal size 12.5 mm (conforms to Table 7 of IS 383:2016 [34])
	12.5 mm	-	98.68	
	10 mm	100	41.32	
	4.75 mm	100	0	
	2.36 mm	90.8	-	
	1.18 mm	76.2	-	
	600 μm	62.3	-	
	300 μm	15.2	-	
	150 μm	0	-	
Specific gravity		2.64	2.78	

3.2. Performance of Binders

The physical characteristics of all binders used for concrete paving blocks are as presented in Table 7. The physical characteristics of CC, AAB-1, and AAB-2 comply with the minimum requirements of OPC 33-grade, making them appropriate to use in manufacturing paving blocks. On the other hand, AAB-3 gained a 28-day CS slightly below the minimum 33 MPa. However, it is noteworthy that all other physical properties of AAB-3 complied with the minimum criteria required. This suggests that despite its minor lag in CS, AAB-3 was still considered fit for incorporation in the concrete mixes for developing paving blocks.

Table 7. Physical properties of some binders used in the current study

Characteristics	Requirements for OPC 33-grade (IS 269:2015 [48])	Binders			
		CC	AAB-1	AAB-2	AAB-3
Fineness (m^2/kg)	≥225	348±2	351± 5	358± 4	362±2
Standard consistency (%)	-	32	29	32	33
Initial setting time (minutes)	≥30	134±6	55± 5	76± 2	88±4
Final setting time (minutes)	≤600	288±8	285± 6	328± 7	420± 4
Compressive strength (MPa)					
(a) 3 days	≥ 16	22.22±0.8	30.58 ± 0.5	24.79 ± 1.6	22.35±1.1
(b) 7 days	≥ 22	29.34±1.4	35.8 ± 0.9	30.38± 0.9	26.06±1.2
(c) 28 days	≥ 33	38.52±0.5	40.00 ±1.1	35.12±1.2	31.24±0.8
Soundness (mm)	≤10	1.2± 0.1	2.0± 0.2	1.8± 0.3	1.4± 0.2

The test results suggest the significance of the SMS/CH ratio in affecting the performance of AABs. An elevated SMS/CH ratio resulted in an increase in the CS of binders. This increment is associated with the development of strength-giving phases, such as calcium alumino silicate hydrate (C-A-S-H) gels, from the hydration of the binders [8,21]. Apart from that, solid activator ratio reduction led to enhanced fineness, enhanced setting time, lower CS, and better soundness of AABs. This, thus, implies that the use of CH as an auxiliary activator is significant in enhancing fineness, retarding setting, and rendering binders sound. This improvement is likely attributed to the very fine particle size of CH, promoting better interactions within the binder matrix [47]. On the other hand, the

results also indicate that raising the proportion of CH in the mix adversely impacted the CS of the binders. Overall, the prolonged setting time and comparable CS of AABs suggested the suitability of binders to be used in making high-performance concrete paving blocks.

3.3. Visual Aspect, Shape and Dimension

The visual attributes, shape, and dimension of the produced paving blocks were examined based on the criteria outlined in IS 15658:2021 [30]. A general visual examination was conducted on individual paving blocks in order to assess their homogeneity and uniformity in form and dimension and, further, the inspection of the flatness and smoothness of their top surfaces. All the paving blocks produced in the duration of this research met the prescribed design requirements without showing any evident deficiency like cracks, delamination, or other serious defects that would compromise their structural integrity.

Table 8. Concrete paving blocks and surface area measurement for all mix designs

Block type	Length, L, mm	Width, W, mm	Thickness, T, mm	Aspect ratio (L/T)	Arris/ Chamfer, mm	Plan area (mm^2)	Wearing face area (mm^2)
Zig-Zag paving blocks	265± 0.5	120± 1	60± 2	4.4± 0.2	5± 0.05	29400	25930

The color of AAB paving blocks was identified as white, whereas CC paving blocks were gray in color, as shown in Figure 5. The specific dimensions and surface areas of the paving blocks can be found in Table 8. It was noted that the tolerances for the length, width, and thickness of the blocks comfortably satisfied the requirement set by IS 15658:2021 [30]. According to the standard, the maximum aspect ratio for paving blocks should be 4; however, the aspect ratio of paving blocks developed here was around 4.4, which is due to the size of the mold used.

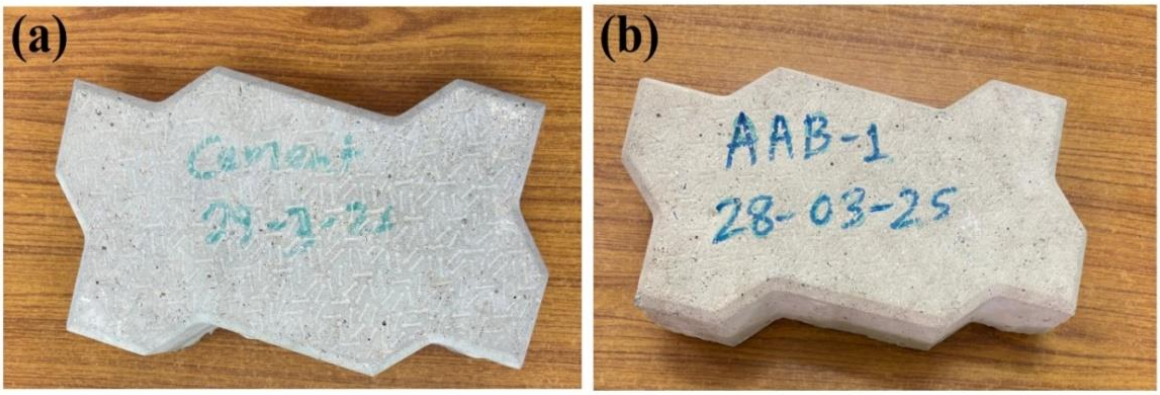

Fig. 5. Visual appearance of CC and AAB paving blocks

3.4. Mechanical Performances

3.4.1. Compressive Strength

The corrected CS of paving blocks was assessed at intervals of 3-, 7-, 14-, and 28-days post-casting, as depicted in Figure 6. The CS of all developed blocks demonstrated an upward trend with the duration of curing. The gain in CS with curing time is primarily because of the fast hydration and the resulting formation of strength-giving phases within the paving blocks. It is worth-noting that AAB-1 blocks, which composed a 14% SMS dosage and an SMS/CH ratio of 2.33, produced the maximum CS at all the ages. Specifically, after 28-days curing, the CS for paving blocks with solid activator ratios of 2.33, 1.50, and 1.00 was recorded at 51.08 MPa, 42.83 MPa, and 38.09 MPa, respectively. These outcomes show that the CS of AAB-1 blocks consistently surpassed that of the CC blocks throughout each stage of the curing process. Moreover, the data suggest that a reduction in the solid activator ratio (SMS/CH) led to a reduction in CS of AAB blocks. The trend may be linked to lesser evolution of strength-giving phases due to the decrease in SMS dosages; however, it is

significant that the strengths achieved remained considerably above the minimum standard requirement of 35 MPa for specified concrete mixtures in paving blocks [30]. In respect to AAB blocks, the binder's hydration starts with the dissolution of solid activators and GGBS particles, resulting in the generation of C-A-S-H gels. Previous research has indicated that C-A-S-H gels are the primary phase contributing to strength in AAB formulations with high-calcium solid precursors [7,49]. Therefore, the strength development observed in AAB blocks can chiefly be linked to the existence and development of these C-A-S-H gels.

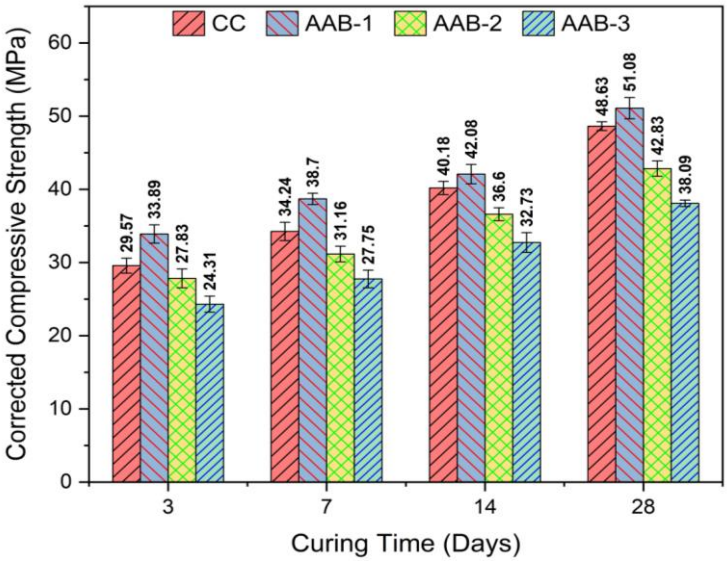

Fig. 6. Corrected compressive strength of paving blocks

The incorporation of CH as a supplementary activator alongside SMS within the alkali-activation system proved advantageous, as there were no indications of efflorescence or shrinkage cracks in the specimens. Furthermore, the inclusion of CH not only facilitated strength progression by providing soluble calcium that interacts with silica and alumina to form C-A-S-H gel but also contributed in enhancing the hardened densities of AAB blocks, thus augmenting their overall strength [47]. The pace of strength development in AAB blocks superseded that of CC blocks. The percentages of strength attainment at 3, 7, and 14 days were recorded at 60%, 70%, and 82%, respectively, relative to their 28-day strength. Conversely, the AAB blocks demonstrated percentages of strength attainment at these intervals of approximately 65%, 74%, and 85%, respectively, when compared to their 28-day CS. The swift gain in CS observed in AAB blocks can be ascribed to the expedited evolution of C-A-S-H gels. This occurrence results upon the rapid dissolution of activators, along with the increased reactivity of GGBS [13,50]. This trend of rapid initial strength development is consistent with previous research, which noted that strength typically increases swiftly during the early stages of curing, followed by a deceleration in later phases [8,45]. The failure patterns of the paving block after compression test, displayed in Figure 2 (a), were similar for both CC and AAB blocks. As vertical loads increased, we noticed lateral expansions in the blocks, which is in line with Poisson's behavior [18].

3.4.2. Tensile Splitting Strength

The TSS of the developed blocks over 3, 7, 14, and 28 days is presented in Figure 7. Similar to the result pattern seen in CS, a consistent increase in TSS with age of curing was seen. Notably, AAB-1 blocks attained the peak TSS of 3.56 MPa at 28-days, considerably surpassing the figures noted for CC blocks and other AAB blocks. The development of early age strength, especially at 3 and 7 days, was less prominent regarding TSS compared to the improvements observed in CS. For CC blocks, data indicate strength increases of 36% and 60% at 3 and 7 days, respectively. Conversely, the AAB blocks showed average strength enhancements of 33% and 58% during these periods. The impact of SMS dosages and the solid activator ratio on split tensile strength mirrored the trend noticed for CS. Remarkably, the mean TSS of all the paving blocks satisfied the minimum mean TSS criterion of 2.97 MPa, as outlined for M35 paving blocks in the standard IS 15658:2021 [30]. Nonetheless, it is

noteworthy that AAB-3 exhibited the lowest TSS, barely meeting the minimum threshold. The post-test failure pattern, as depicted in Figure 2 (b), generally involves the blocks splitting approximately into two equal halves along their length. This mode of failure was consistently observed in both CC and AAB blocks.

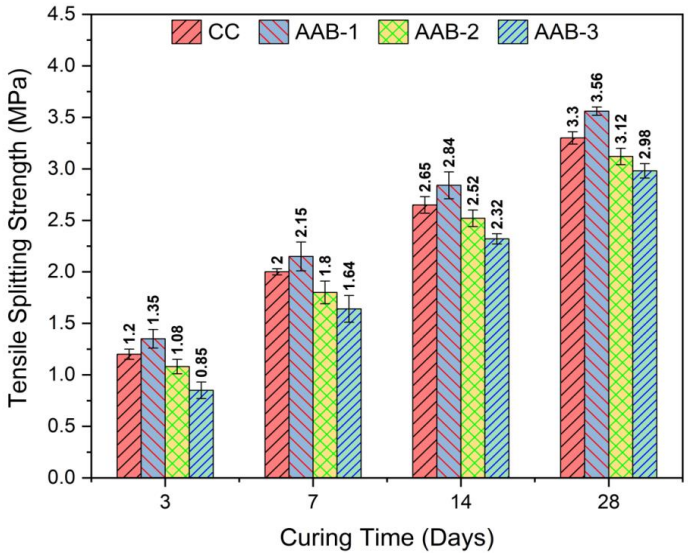

Fig. 7. Tensile splitting strength of paving blocks

3.4.3. Flexural Strength

The FS of the developed blocks assessed at 3, 7, 14, and 28 days is shown in Figure 8. With an increase in the curing period, both CC and AAB paving blocks developed a significant gain in terms of FS. Especially, the AAB-1 blocks have achieved a very high performance with FS of 8.44 MPa at 28-days curing, which is a much higher strength than the CC blocks. However, like before in relation to TSS, the early enhancements in FS at both 3 and 7 days were less pronounced than the evident strides in their CS. In other words, CC blocks presented a 15% higher strength at 3 days and a 48% higher strength at 7 days.

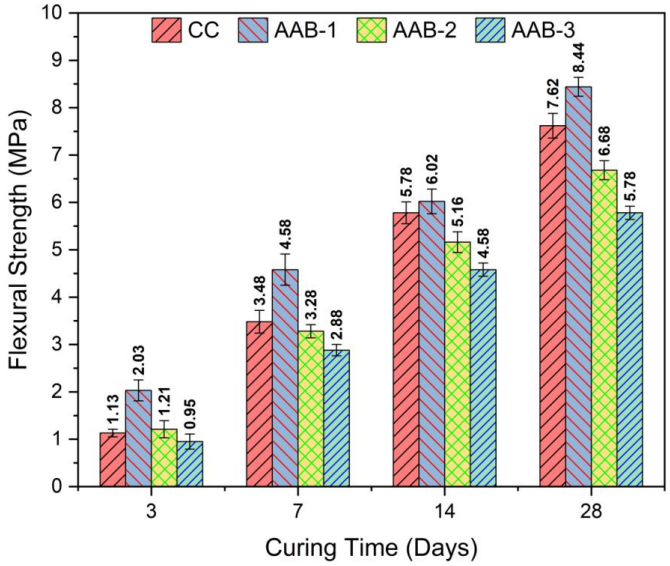

Fig. 8. Flexural strength of paving blocks

The AAB blocks showed average increases of 19% and 51% over the same periods. The way SMS dosages and the solid activator ratio affect FS were consistent with their impact on compressive and split tensile strengths. It's noteworthy that the mean FS of all the blocks produced met the minimum average requirement of 3.85 MPa for M35 paving blocks, as outlined in IS 15658:2021

[30]. Figure 2 (c) illustrates that during the evaluation of flexural performance, the observed failure modes were characteristic of flexural failure, manifesting as distinct crack formations with the blocks nearly splitting into two halves.Figure 9 displays the correlation between CS and TSS, representing R^2 values for all paving blocks varying from 0.9284 to 0.9713. This indicates a strong concurrence, suggesting that an enhancement in CS is accompanied by a corresponding rise in the TSS of the paving blocks. Similarly, Figure 10 presents the association between CS and FS, exhibiting R^2 values ranging from 0.9433 to 0.9501. This again shows the strong relationship between these two properties. The positive trend evident in the linear regression for both scenarios clearly **point** to the fact that higher CS is linked with an improvement in TSS and FS, thus indicating a uniform trend throughout all the assessments. In similar research studies [19,24], linear relationships between CS with TSS and CS with FS were established for AAB-based concrete blocks. TSS and FS increase as CS increases, indicating interdependence between these mechanical properties.

3.4.4. Relationship Between Mechanical Properties

To obtain the relation between mechanical properties, a linear regression analysis was conducted to find the relationship between CS with TSS, as well as FS.

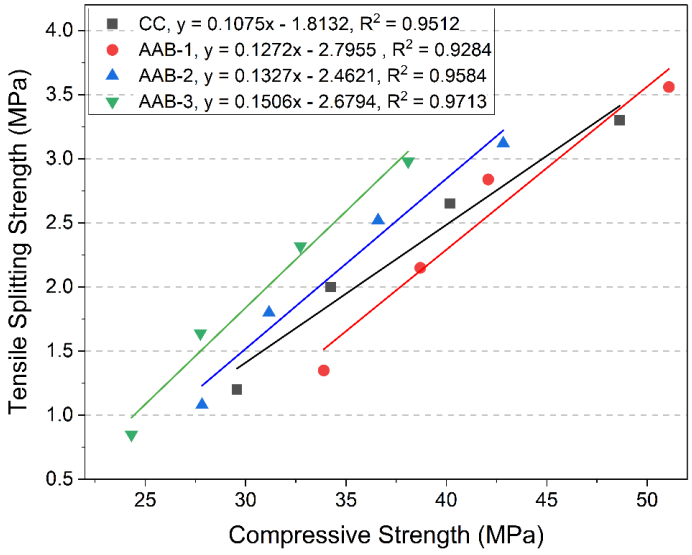

Fig. 9. Correlation between compressive strength and tensile splitting strength

3.5. Density and water absorption

The densities of developed paving blocks were assessed based on mass-to-volume ratios, as displayed in Figure 11. The density of all paving blocks was found to range from 2490 to 2648 kg/m^3. Notably, the density of the CC paving blocks exceeded that of all other blocks. The slightly lower density of AAB blocks compared to CC blocks might stem from the lower specific gravity of AAB. Within the AAB blocks, the similar densities could be linked to the formation of phases that boost strength, along with the existence of finer CH particles in the concrete matrix [47,49]. An increase in SMS dosage was accompanied by a rise in bulk density. Furthermore, there was a clear link between the bulk density and the CS of the AAB blocks; higher density of paving blocks resulted in higher strength. Previous studies [24] also illustrated that the density of the AAB blocks varied from 2350-2400 kg/m^3, similar to current study. The same linear relationship between the density of the AAB blocks and the CS was also found in a previous study [19].

Figure 11 presents the values of water absorption in prepared paving blocks. The outcomes show that the water absorption capacity for CC blocks was observed at 3.09%. This is significantly lower than that of all AAB blocks, with the AAB-3 block having the highest capacity at 4.95%. The result shows there is a clear reverse correlation between density and water absorption. The lower the density of the blocks, the higher is the tendency for water absorption. This is most likely because there are available small pores for water penetration in the concrete matrix. However, the findings

show that all the tested blocks met the water absorption requirements, set at 6% by IS 15658:2021 [30]. In a similar study [24], water absorption of the order of 3.80 % was observed for FA-based AAB paving blocks, which is close to the present observed value. Also, a value of 2.85-3.03 % was observed for FA-GGBS-based paving blocks in similar research [2].

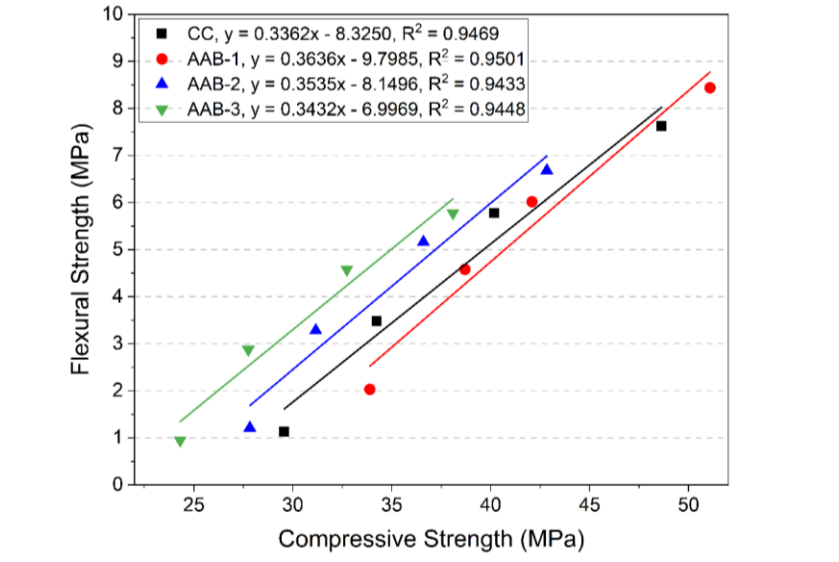

Fig. 10. Correlation between compressive strength and flexural strength

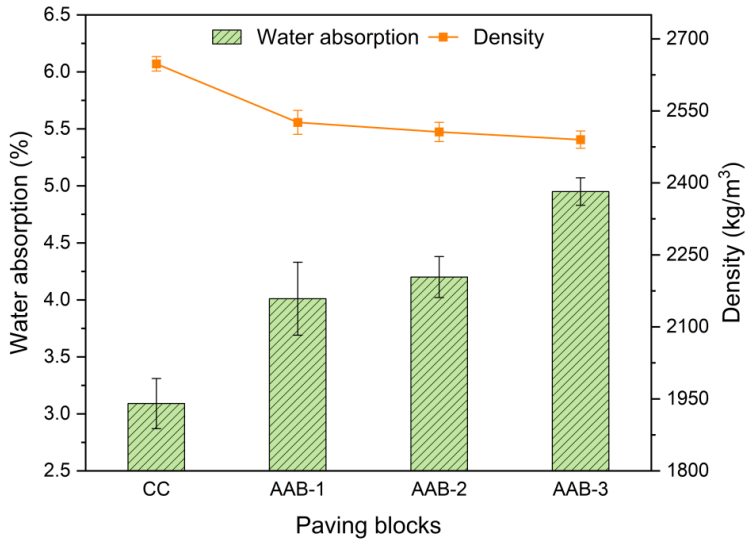

Fig. 11. Water absorption and density of developed paving blocks

For FA-Silica fume-based AAB blocks, a lower value of 1.98 % was observed in a past work [26]. In another instance [51], water absorption in cement pervious concrete for paving was found to be between 3.79% and 5.29%, a value very similar to this study. This indicates AAB blocks have low water absorption, therefore satisfying the regulatory standards. This conformity also reflects the performance of the blocks in various applications where water resistance is of great concern.

3.6. Abrasion Resistance

Figure 12 presents the findings of the abrasion resistance of paving blocks, conducted at a maturity time of 28-days. The average abrasion resistance, expressed as volume loss, ranged from 7522 to 8906 mm^3 per 5000 mm^2 across all paving blocks. It can be observed that all blocks showed abrasion resistance values below the permissible maximum value of 18,000 mm^3 per 5,000 mm^2, which is a requirement for all concrete paving blocks according to IS 15658:2021 [30]. Among the different variations tested, the AAB-1 blocks demonstrated better abrasion resistance compared to the CC blocks and other AAB types. This indicates that lowering the ratio of SMS/CH in AAB blocks

led to a decrease in their abrasion resistance. The enhanced resistance to abrasion of AAB blocks is attributed to their compact microstructure and superior bonding with aggregate particles [24]. Furthermore, the integration of very fine CH particles within the alkali-activated matrix fortifies the interfacial bond, enhancing the linkage between the aggregate and the gel, subsequently elevating abrasion resistance. Earlier research [2,24] had shown the abrasion resistance of two-part AAB blocks as ~10000-13000 mm^3 per 5,000 mm^2, which is greater than that of the present study. In another similar study [26], better abrasion resistance of 2710 mm^3 per 5,000 mm^2 was indicated for two-part FA-silica fume-based AAB blocks. The abrasion resistance values obtained in this work lies within these range. This indicates their potential utilization in pedestrian and low vehicular traffic applications.

3.7. Acid Attack Resistance

The result of acid resistance testing, which was carried out using a 5% sulfuric acid, is presented in Figure 12. The result indicated that CC blocks were much more adversely affected by acid exposure. Conversely, AAB blocks were much more resistant to acidic exposure, as depicted in Figure 13. The CC blocks suffered the most significant loss in CS, registering a loss of 5.52%. The AAB-1 blocks, however, reported the minimum loss in strength, which was 3.78%.

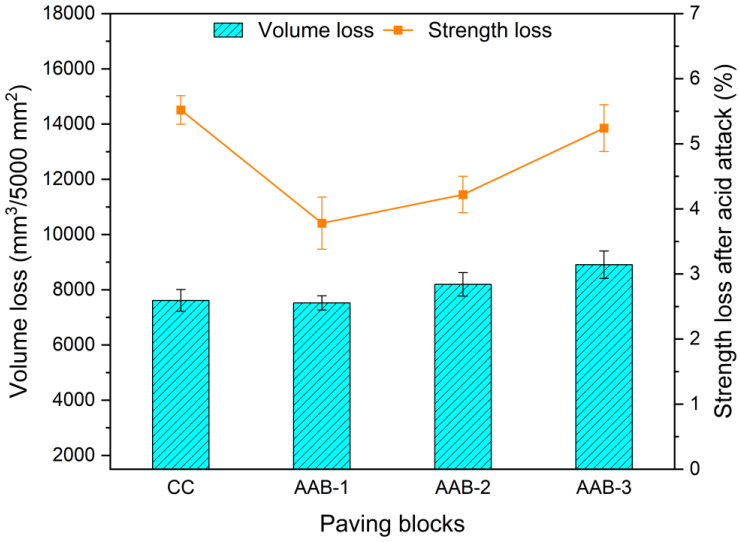

Fig. 12. Abrasion and acid resistance of the produced paving blocks

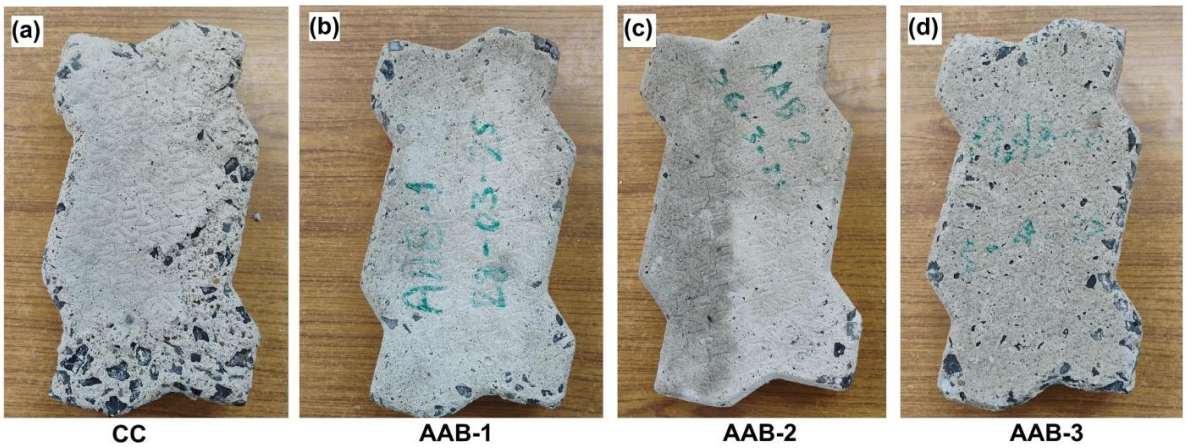

Fig.13. Visual appearance of the paving blocks after acid exposure at 28-days

A previous study [2] has identified the higher acid resistance (~2.15%) of AABs produced with GGBS activated by a mixture of liquid activators. In another study [24] on FA-based AAB paving blocks, an acid resistance of approximately 4.50 % strength loss was found. These results clearly demonstrate that developed AAB blocks possess enhanced durability compared to CC blocks under

acidic environments. It highlights their prospective application in areas where resistance to chemical degradation is essential, especially in industrial settings like chemical plants, food and beverage plants, sewage and wastewater treatment plants, and manufacturing plants where acids are often used or spilled.

3.8. Summary of the Performance of AAB-Based Concrete Paving Blocks

Table 9 presents a summary of major findings on the development of AAB paving blocks, while also providing a thorough comparison with performance data from previous scholarly studies conducted over the past few years. Notably, the results obtained from the current study revealed that concrete paving blocks, developed using GGBS-based one-part AABs, showed performance metrics that are not only comparable to but in certain instances may even surpass those observed in two-part AAB formulations that utilize a variety of solid precursors and activators in their composition.

Table 9. Summary of AAB-based concrete paving blocks developed in recent years

AAB type	Solid precursor	Activators & their ratio	Curing method	Paving block grade	CS 28 d (MPa)	TSS 28 d (MPa)	FS 28d (MPa)	WA (%)	Ref.
Two-part AAB	FA-GGBS	SS+SH, 1.5	Ambient	M40	72.13	3.80	6.63	3.03	[2]
	FA-GGBS	SS+SH, 1.5	Ambient	M50	75.35	4.23	6.36	2.85	[2]
	FA-BKRHA	SS+SH, 2.5	Sundried (45 °C)	M40	44.30	3.30	7.60	4.40	[24]
	FA	SS+SH, 2.5	Sundried (45 °C)	M40	43.50	3.10	7.10	3.80	[24]
	BA-GGBS	SS+SH, 2.5	Ambient	M30	57.34	-	-	0.76	[25]
	BA-GGBS	SS+SH, 2.5	Ambient	M35	59.58	-	-	0.28	[25]
	FA	SS+SH, 1.25	60 °C	M35	52.33	-	5.10	2.18	[26]
	FA-SF	SH	60 °C	M35	47.54	-	5.07	1.98	[26]
	FA-GGBS	SS+SH, 2.5	70 °C	M35	41.60	4.70	6.80	5.50	[27]
	FA	SS+SH, 2.5	70 °C	-	-	-	3.80#	5.60	[31]
One-part AAB	GGBS-FA	SMS	Ambient	Pressed block	18.70	5.10	-	2.90	[19]
	GGBS	SMS	Ambient	Pressed block	28.00	-	-	-	[18]
	GGBS	SMS+CH, 2.33	Water	M35	51.08	3.56	8.44	4.01	Current
	GGBS	SMS+CH,1.50	Water	M35	42.83	3.12	6.68	4.20	Current
	GGBS	SMS+CH,1.00	Water	M35	38.09	2.98	5.78	4.95	Current

BKRHA- Brick kiln rice husk ash, BA- Bottom ash, SF-Silica fume, SS-Sodium silicate solution, SH-Sodium hydroxide solution, WA-water absorption, Ref.-References, #7-days flexural strength.

This research distinctly emphasizes the substantial potential inherent in the utilization of one-part AABs for the production of paving blocks, which can be manufactured through processes that are strikingly similar to those employed in the conventional production of cement-based concrete paving blocks.

3.9. Environmental Benefits

To assess the environmental advantages of one-part AAB blocks compared to traditional concrete blocks, it was essential to examine the environmental effects of the developed blocks. Therefore, the carbon footprint of all the components present in the concrete mixes was evaluated in forms of Global Warming Potential (GWP). The GWP assessment was constrained to the manufacture of blocks with the designed mix ratios, excluding other life cycle stages. The analysis presented employs a highly streamlined method to measure the ecological benefits of AAB blocks compared

to CC blocks. The GWP contributions of all ingredients in the binder, as well as the concrete mix, were computed based on established CO_2-equivalent values (in kg CO_2-eq/kg). The required data regarding GWP contributions of the materials were utilized from several previous studies [19,52–56]. The subsequent GWP information was used for the evaluation:

- OPC: The GWP of OPC is considerably high, mainly because of the calcination and significant energy expenditure during the production of cement clinker, and it is estimated to be approximately 0.85 kg CO_2-eq/kg.
- FA: It is an industrial by-product, obtained from coal combustion, it generally possesses a very less emissions about 0.01 kg CO_2-eq/kg.
- GGBS: Another industrial by-product that belongs to the steel industry, GGBS has a less GWP of about 0.07 kg CO_2-eq/kg.
- SMS: The manufacturing of sodium metasilicate is an energy-demanding process, typically resulting in a considerably high GWP, around 0.80 kg CO_2-eq/kg.
- CH: The production of hydrated lime is likewise an energy-demanding procedure necessitating limestone calcination similar to OPC, thereby possessing a higher emission, near 0.94 kg CO_2-eq/kg.
- Aggregate: As natural materials, fine and coarse aggregates are considered to have a very less GWP of about 0.05 kg CO_2-eq/kg each.
- Water: Since water is a natural resource, it essentially has a negligible GWP.

Table 10. Global warming potential of paving blocks per cubic meter of concrete mix, expressed in kg CO_2-eq/m^3

Mix ID	OPC	GGBS	FA	SMS	CH	Fine Agg.	Coarse Agg.	W	Total GWP (T.G.)	% GWP reduction* with respect to OPC as binder
CC	140.57	9.61	1.47	-	-	32.625	59.625	0	243.90	48.63%
AAB-1	-	25.20	-	50.40	25.38	32.625	59.625	0	193.23	59.30%
AAB-2	-	25.20	-	43.20	33.84	32.625	59.625	0	194.49	59.03%
AAB-3	-	25.20	-	36.00	42.30	32.625	59.625	0	195.75	58.77%
OPC (Ref.)	382.50	-	-	-	-	32.625	59.625	0	474.75	-

* GWP reduction % = [(474.75-T.G.)/474.75]x100, Agg.- Aggregate, W-Water, Ref.-Reference binder

Based on the aforementioned data, the GWP calculations were completed and displayed in Table 10. The GWP assessment reveals the subsequent environmental impacts of the materials utilized in this research. Assuming identical mix proportions and employing OPC as the binder, the GWP of OPC-based paving blocks would amount to 474.75 kg CO_2-eq/m^3 (determined as shown in Table 10). Relative to OPC-based blocks, the CC paving blocks exhibited a reduced overall GWP, approximately 49% less. When employing AAB paving blocks, the overall GWP has decreased further, reaching about 59% for all AAB blocks in comparison to those based on OPC, as shown in Figure 14a. Compared to CC paving blocks, the GWP was reduced by 10% in the AAB blocks. The difference in the ratio of SMS and CH equally has the same effect on GWP, as they have high and equal GWP values. The study shows that the one-part AAB paving blocks have lower carbon footprints and thus have environmental benefits compared to conventional paving blocks.

3.10. Cost-Effectiveness

In this research, efforts were undertaken to create concrete paving blocks by substituting traditional cement with one-part AABs. Additionally, other components like natural river sand, coarse aggregate, and water were consistently used across all binders. To assess the cost-effectiveness of the paving blocks, only the expenses related to the binders were compared and are displayed in Table 11. The currency used in Table 11 is USD ($). The estimated unit costs of GGBS, SMS, and CH were 0.0291, 0.326, and 0.140 $ per kilogram, according to the current market rates in India. The cost of CC and OPC (33-grade) was approximately 4.372 and 4.547 $ for a 50 kg bag

from major manufacturers in India. These costs, however, differ greatly based on the manufacturer, location, shipping, and quantity of supply needed. The prices selected here are an average of the going rates for the materials' bulk supply on the market. A cost analysis was conducted and presented using this data for a designed binder quantity of 450 kg/m^3.

Table 11. Cost calculations for binders to produce paving blocks per cubic meter of concrete mix

Mix ID	Cost of binders' ingredients per 50 kg			Cost of binder per 50 kg	Total cost (T.C.) for 450 kg/m^3 of binder	% Cost reduction with respect to OPC as binder [(40.923-T.C.)/40.923]x100
	GGBS (0.0291 $/kg)	SMS (0.326 $/kg)	CH (0.140 $/kg)			
CC	-	-	-	$4.372	$39.348	3.85%
AAB-1	$1.164	$2.282	$0.420	$3.866	$34.791	14.98%
AAB-2	$1.164	$1.956	$0.560	$3.680	$33.116	19.08%
AAB-3	$1.164	$1.630	$0.700	$3.494	$31.442	23.17%
OPC (Ref.)	-	-	-	$4.547	$40.923	-

[1 US$ = 85.77 INR (₹) in June 2025]

The research indicates that the use of AABs can provide to an economic saving of costs by approximately 11-19% relative to CC. Furthermore, relative to 33-grade OPC, AABs can lead to an expenditure saving of approximately 15-23% (Figure 14b). Thus, concrete paving blocks can be built as economically using AABs, provided that everything else is equal. Thus, the paving blocks created offer a compelling option for producing budget-friendly and sustainable pavement solutions suitable for various uses, ranging from areas with no traffic to regions with low traffic.

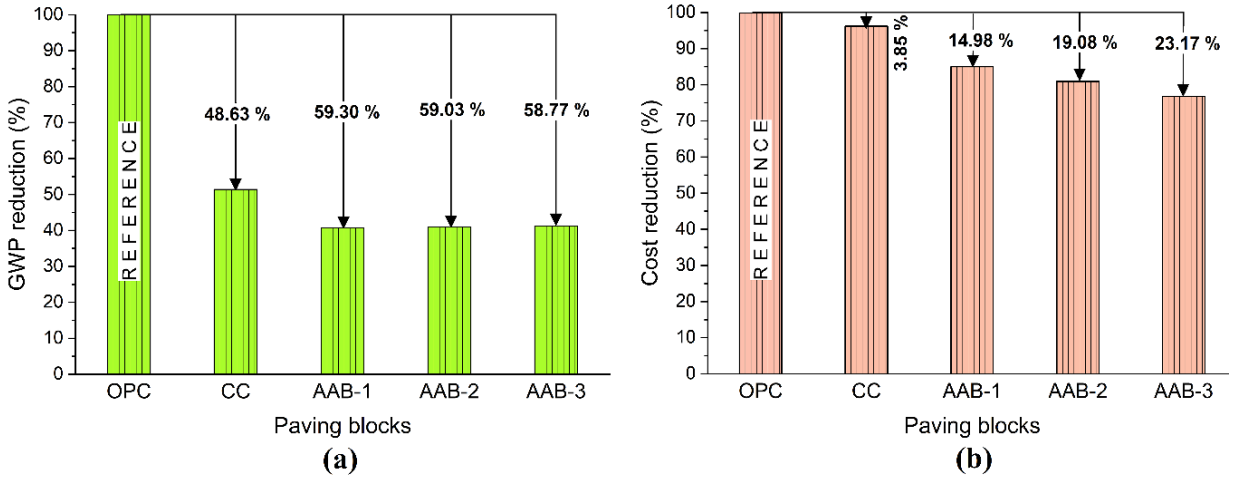

Fig. 14. (a) GWP reduction and (b) cost-effectiveness of developed paving blocks

4. Conclusions

In conclusion, the use of replacement binders, one-part AABs, particularly in the production of concrete paving blocks, is extensively addressed, and the test results indicate several benefits over traditional pavement blocks, as explained below:

- The effectiveness of AABs as a binder in the production of concrete paving blocks is well established by the study results, wherein all AABs performed to or even surpassed key performance requirements, although AAB-3 had relatively lower compressive strength.
- The research emphasizes the significance of the ratio of sodium metasilicate (SMS) to calcium hydroxide (CH) in the determination of binder characteristics, and that a higher ratio leads to improved strength and durability characteristics of blocks.

- Several tests revealed that all AAB blocks had improved performance, better than that of regular blocks, in strength and durability, especially in compressive, tensile splitting, and flexural strengths, as well as their abrasion and acid resistance. Notably, AAB-1 paving block consistently outshines traditional concrete blocks when it comes to strength and durability.
- The AAB paving blocks possess up to 59% lower CO2 emissions compared to their conventional paving blocks, along with a significantly reduced GWP. The cost analysis supports this as well, showing that making AAB blocks can lead to savings of 15% to 23% compared to traditional blocks. This makes them both environmentally friendly and economically efficient at the same time.

Overall, the research outcomes indicate that the utilization of a one-pat alkali-activated binder is a superior method of producing durable and affordable concrete paving blocks. The products are environmentally friendly and very suitable for use in non-traffic to low-traffic pavement applications.

Acknowledgement

The authors acknowledge the faculties and staffs of Department of Civil Engineering, National Institute of Technology Patna for their support. The authors extend their appreciation to the Principal, Government Polytechnic Katihar for his kind support. Additionally, they recognize Nishka Research Pvt. Ltd., Hyderabad for facilitating material characterizations.

References

[1] Industrial wastes as alternative binders in precast concrete elements. In: The path to green concrete. Elsevier; 2024. p. 151-70. https://doi.org/10.1016/B978-0-443-19165-7.00003-4

[2] Srividya T, Rajkumar PRK. Mechanical and durability properties of alkali-activated binders based paver blocks derived from secondary sources. Case Stud Constr Mater. 2022;17:e01561. https://doi.org/10.1016/j.cscm.2022.e01561

[3] Interlocking concrete pavers market size, share, competitive landscape and trend analysis report by thickness, by application, by end-user: global opportunity analysis and industry forecast, 2023–2032. Allied Market Research; 2023. Available from: https://www.alliedmarketresearch.com/interlocking-concrete-pavers-market-A131494 [Accessed 2025 May 30].

[4] Massoumi Nejad B, Enferadi S, Andrew R. A comprehensive analysis of process-related CO2 emissions from Iran's cement industry. Cleaner Environ Syst. 2025;16:100251. https://doi.org/10.1016/j.cesys.2024.100251

[5] GCCA India-TERI. Decarbonization roadmap for the Indian cement sector: net-zero CO2 by 2070. 2025. Available from: https://www.teriin.org/policy-brief/decarbonization-roadmap-indian-cement-sector-net-zero-co2-2070 [Accessed 2025 May 28].

[6] Ren J, Sun H, Li Q, Li Z, Ling L, Zhang X, et al. Experimental comparisons between one-part and normal (two-part) alkali-activated slag binders. Constr Build Mater. 2021;309:125177. https://doi.org/10.1016/J.CONBUILDMAT.2021.125177

[7] Yin K, Jiang Y, Pan Y, Li Z, Xie N, Meng J. Properties comparison of one-part and two-part alkali-activated slag pastes. Case Stud Constr Mater. 2024;e03884. https://doi.org/10.1016/j.cscm.2024.e03884

[8] Segura IP, Luukkonen T, Yliniemi J, Sreenivasan H, Damø AJ, Jensen LS, et al. Comparison of one-part and two-part alkali-activated metakaolin and blast furnace slag. J Sustain Metall. 2022;8:1816-30. https://doi.org/10.1007/s40831-022-00606-9

[9] Ahmad MR, Chen B, Shah SFA. Influence of different admixtures on the mechanical and durability properties of one-part alkali-activated mortars. Constr Build Mater. 2020;265:120320. https://doi.org/10.1016/j.conbuildmat.2020.120320

[10] Askarian M, Tao Z, Samali B, Adam G, Shuaibu R. Mix composition and characterisation of one-part geopolymers with different activators. Constr Build Mater. 2019;225:526-37. https://doi.org/10.1016/j.conbuildmat.2019.07.083

[11] Luukkonen T, Abdollahnejad Z, Yliniemi J, Kinnunen P, Illikainen M. One-part alkali-activated materials: a review. Cem Concr Res. 2018;103:21-34. https://doi.org/10.1016/j.cemconres.2017.10.001

[12] Adesanya E, Ohenoja K, Di Maria A, Kinnunen P, Illikainen M. Alternative alkali-activator from steel-making waste for one-part alkali-activated slag. J Clean Prod. 2020;274:123020. https://doi.org/10.1016/j.jclepro.2020.123020

[13] Elzeadani M, Bompa DV, Elghazouli AY. One part alkali activated materials: a state-of-the-art review. J Build Eng. 2022;57:104871. https://doi.org/10.1016/j.jobe.2022.104871

[14] Coppola L, Coffetti D, Crotti E, Gazzaniga G, Pastore T. The durability of one-part alkali-activated slag-based mortars in different environments. Sustainability. 2020;12:3561. https://doi.org/10.3390/su12093561
[15] Kumar A, Kumar V, Prasad B. Strength development and flexural behavior of reinforced concrete beam using one-part alkali-activated binder. Constr Build Mater. 2021;281:122619. https://doi.org/10.1016/j.conbuildmat.2021.122619
[16] Adesina A, Das S. Drying shrinkage and permeability properties of fibre reinforced alkali-activated composites. Constr Build Mater. 2020;251:119076. https://doi.org/10.1016/j.conbuildmat.2020.119076
[17] Kramarič D, Grubeša IN, Torič N, Ribič R, Mijatovič N, Vasič MV. Fire resistance of crushed brick-based alkali-activated mortars. Civ Eng J. 2025;11:1331-52. https://doi.org/10.28991/CEJ-2025-011-04-05
[18] Rashid K, Raoof MN, Daud M, Wang Y, Ju M. One-part alkali activated binder activated by sodium metasilicate and ternary-factored sustainability of structural block. Structures. 2024;68:107108. https://doi.org/10.1016/j.istruc.2024.107108
[19] Jameel M, Suteerasak T, Chumpol P, Puttiwongrak A, Sae-Long W, Sukontasukkul P. Properties of one-part geopolymer pedestrian blocks made using 100% waste materials. Case Stud Constr Mater. 2025;22:e04538. https://doi.org/10.1016/j.cscm.2025.e04538
[20] Haruna S, Mohammed BS, Wahab MMA, Kankia MU, Amran M, Gora AM. Long-term strength development of fly ash-based one-part alkali-activated binders. Materials. 2021;14:4160. https://doi.org/10.3390/ma14154160
[21] Dong M, Elchalakani M, Karrech A. Development of high strength one-part geopolymer mortar using sodium metasilicate. Constr Build Mater. 2020;236:117611. https://doi.org/10.1016/j.conbuildmat.2019.117611
[22] Rasuli MI, Tajunnisa Y, Yamamura A, Shigeishi M. A consideration on the one-part mixing method of alkali-activated material: problems of sodium silicate solubility and quick setting. Heliyon. 2022;8:e08783. https://doi.org/10.1016/j.heliyon.2022.e08783
[23] Sood D, Hossain KMA. Optimizing precursors and reagents for the development of alkali-activated binders in ambient curing conditions. J Compos Sci. 2021;5:59. https://doi.org/10.3390/jcs5020059
[24] Mahdi SN, Babu R DV, Hossiney N, Abdullah MMAB. Strength and durability properties of geopolymer paver blocks made with fly ash and brick kiln rice husk ash. Case Stud Constr Mater. 2022;16:e00800. https://doi.org/10.1016/j.cscm.2021.e00800
[25] Revathi V, Thaarrini J, Rao MV. A prospective study on alkali activated bottom ash-GGBS blend in paver blocks. Int J Civil Architect Sci Eng. 2014;8:53–60. Available from: https://www.researchgate.net/publication/301618646_A_Prospective_Study_on_Alkali_Activated_Bottom_Ash-GGBS_Blend_in_Paver_Blocks_V_Revathi_J_Thaarrini_M_Venkob_Rao
[26] Bajpai R, Soni V, Shrivastava A, Ghosh D. Experimental investigation on paver blocks of fly ash-based geopolymer concrete containing silica fume. Road Mater Pavement Des. 2023;24:138–55. https://doi.org/10.1080/14680629.2021.2012236
[27] Ganesh AC, Mohana R, Loganathan P, Kumar VM, Kırgız MS, Nagaprasad N, Ramaswamy K. Development of alkali activated paver blocks for medium traffic conditions using industrial wastes and prediction of compressive strength using random forest algorithm. Sci Rep. 2023;13:15152. https://doi.org/10.1038/s41598-023-42318-4
[28] Meshram S, Yerawar S, Fopare A, Nimbarte S, Hadke R, Derkar P, Rathod R. Development of paver blocks using cupola slag and fly ash. IOP Conf Ser Earth Environ Sci. 2024;1409:012003. https://doi.org/10.1088/1755-1315/1409/1/012003
[29] Rajan MRR, Rajalinggam D, Narayanan K, Ramasamy S. Eco-friendly paver blocks: repurposing plastic waste and foundry sand. Matéria (Rio J). 2025;30:e20240707. https://doi.org/10.1590/1517-7076-rmat-2024-0707
[30] IS 15658:2021. Concrete paving blocks — Specification (First Revision). 2021.
[31] Lăzărescu A-V, Ionescu BA, Hegyi A, Florean C. Alkali-activated fly ash based geopolymer paving blocks: green materials for future conservation of resources. Int J Civil Struct. 2022;13:175–86. Available from: https://ijcs.ro/public/IJCS-22-13_Lazarescu.pdf
[32] Abdollahnejad Z, Mastali M, Luukkonen T, Kinnunen P, Illikainen M. Fiber-reinforced one-part alkali-activated slag/ceramic binders. Ceram Int. 2018;44:8963–76. https://doi.org/10.1016/j.ceramint.2018.02.097
[33] IS 16415:2015. Composite cement — Specification. 2015.
[34] IS 383:2016 (Reaffirmed 2021). Coarse and fine aggregate for concrete specification (Third Revision). 2016.
[35] IS 456:2000 (Reaffirmed 2021). Plain and reinforced concrete code of practice (Fourth Revision). 2000.
[36] IS 10262:2019. Concrete mix proportioning guidelines (Second Revision). 2019.
[37] IS 1727:1967. Methods of test for pozzolanic materials. 1967.

[38] IS 2386 (Part I):1963 (Reaffirmed 2021). Methods of Test for Aggregates for Concrete Part I: Particle Size and Shape. 1963.
[39] IS 2386 (Part III):1963 (Reaffirmed 2021). Methods of Test for Aggregates for Concrete Part III: Specific Gravity, Density, Voids, Absorption and Bulking. 1963.
[40] IS 4031 (Part 2):1999. Methods of physical tests for hydraulic cement, Part 2: Determination of fineness by specific surface by Blaine air permeability method. 1999.
[41] IS 4031 (Part 4):1988. Methods of physical tests for hydraulic cement, Part 4: Determination of consistency of standard cement paste. 1988.
[42] IS 4031 (Part 5):1988. Methods of physical tests for hydraulic cement, Part 5: Determination of initial and final setting times. 1988.
[43] IS 4031 (Part 6):1988. Methods of physical tests for hydraulic cement, Part 6: Determination of compressive strength of hydraulic cement (other than masonry cement). 1988.
[44] IS 4031 (Part 3):1988. Methods of physical tests for hydraulic cement, Part 3: Determination of soundness. 1988.
[45] Zhao Q, Ma C, Huang B, Lu X. Development of alkali activated cementitious material from sewage sludge ash: two-part and one-part geopolymer. J Clean Prod. 2023;384. https://doi.org/10.1016/j.jclepro.2022.135547
[46] Luukkonen T, Sreenivasan H, Abdollahnejad Z, Yliniemi J, Kantola A, Telkki V-V, Kinnunen P, Illikainen M. Influence of sodium silicate powder silica modulus for mechanical and chemical properties of dry-mix alkali-activated slag mortar. Constr Build Mater. 2020;233:117354. https://doi.org/10.1016/j.conbuildmat.2019.117354
[47] Ouyang S, Chen W, Zhang Z, Li X, Zhu W. Experimental study of one-part geopolymer using different alkali sources. J Phys Conf Ser. 2020;1605:012155. https://doi.org/10.1088/1742-6596/1605/1/012155
[48] IS 269:2015. Ordinary Portland Cement — Specification. 2015.
[49] Gao X, Yu QL, Brouwers HJH. Reaction kinetics, gel character and strength of ambient temperature cured alkali activated slag–fly ash blends. Constr Build Mater. 2015;80:105–15. https://doi.org/10.1016/j.conbuildmat.2015.01.065
[50] Luukkonen T, Abdollahnejad Z, Yliniemi J, Kinnunen P, Illikainen M. Comparison of alkali and silica sources in one-part alkali-activated blast furnace slag mortar. J Clean Prod. 2018;187:171–79. https://doi.org/10.1016/j.jclepro.2018.03.202
[51] Barišić I, Grubeša IN, Vasić M, Janaćković A. Assimilating nanographene into the pervious concrete — surface treatment for enhanced paving performance. Case Stud Constr Mater. 2025;23:e04917. https://doi.org/10.1016/j.cscm.2025.e04917
[52] Ecoinvent. Ecoinvent database (Version 3.8). Swiss Centre for Life Cycle Inventories; 2018. Available from: https://www.ecoinvent.org
[53] Sphera Solutions. GaBi database (Version 2023.1). Sphera Solutions GmbH; 2023. Available from: https://www.gabi-software.com
[54] Ji X, Wang X, Zhao X, Wang Z, Zhang H, Liu J. Properties, microstructure development and life cycle assessment of alkali-activated materials containing steel slag under different alkali equivalents. Materials. 2023;17:48. https://doi.org/10.3390/ma17010048
[55] Peng Y-Q, Zheng D-P, Pan H-S, Yang J-L, Lin J-X, Lai H-M, Wu P-Z, Zhu H-Y. Strain hardening geopolymer composites with hybrid POM and UHMWPE fibers: analysis of static mechanical properties, economic benefits, and environmental impact. J Build Eng. 2023;76:107315. https://doi.org/10.1016/j.jobe.2023.107315
[56] Laveglia A, Sambataro L, Ukrainczyk N, De Belie N, Koenders E. Hydrated lime life-cycle assessment: current and future scenarios in four EU countries. J Clean Prod. 2022;369:133224. https://doi.org/10.1016/j.jclepro.2022.133224